STRUCTURE OF TURBULENT FLOW THROUGH A RECTANGULAR CHANNEL
ROTATING ABOUT A TRANSVERSE AXIS

V. V. Ris, E. M. Smirnov,
and S. A. Smirnov

UDC 532.517.4

Developed laminar flow and instability phenomena in a rotating channel with a square cross section were studied in [1]. For the turbulent regime measurements of the developed field of the longitudinal velocity component have been made for only one (central) plane [2]. Numerical modeling of turbulent flow was carried out in [3, 4], but the turbulence model used is limited to low values of the rotation parameter.

Below we present the results of measurement of the fields of averaged velocity and the intensity of pulsations of the longitudinal component in flow through a square channel rotating about a transverse axis. The effects of the direct action of the Coriolis force on the turbulence are analyzed on the basis of a well-known, semiempirical, second-order model. A number of general features of the structure of turbulent flows through rectangular channels with a ratio of sides of the cross section on the order of one are discussed.

1. Theoretical Analysis

The variations of the characteristics of averaged and pulsation motions caused by rotation are due entirely to the Coriolis force for isothermal flows. Two main effects of its action are known [5]. The first of them consists in the additional turbulization or, conversely, stabilization of the flow. This effect is displayed in "pure" form in plane-parallel flows for which the plane is normal to the axis of rotation [6]. The second effect consists in the formation of secondary (transverse) flows with a considerable counterinfluence on the flow in the main direction. As a result, for sufficiently rapid rotation of the channel a core is isolated in the developed stream in which the flow characteristics vary little along the direction parallel to the axis of rotation. The core fills a large part of the channel cross section and can be considered approximately as a plane-parallel flow.

Keeping in mind the necessity of analyzing experimental data, we consider a semiempirical second-order model of turbulence in application to plane-parallel rotating flows.

We write the general form of the exact equations of transfer of the components of the Reynolds stress tensor for quasisteady turbulent flow in the rotating Cartesian coordinate system x_1, x_2, x_3:

$$U_n \partial \langle u_i u_j \rangle / \partial x_n = P_{ij} + G_{ij} + \Phi_{ij} - E_{ij} - D_{ij}. \tag{1.1}$$

Here P_{ij} and G_{ij} are terms expressing the generation of stresses due to deformations of the averaged velocity field and the action of Coriolis forces:

$$P_{ij} = -\langle u_i u_n \rangle \partial U_j / \partial x_n - \langle u_j u_n \rangle \partial U_i / \partial x_n, $$
$$G_{ij} = 2\omega_p (\varepsilon_{ipq} \langle u_j u_q \rangle + \varepsilon_{jpq} \langle u_i u_q \rangle). \tag{1.2}$$

We use the model representations of [7] for the terms reflecting the interaction of pressure pulsations with the velocity field (Φ_{ij}) and the viscosity effects (E_{ij}),

$$\Phi_{ij} = -c_1 \frac{\varepsilon}{k} \left(\langle u_i u_j \rangle - \frac{2}{3} \delta_{ij} k \right) - c_2 \left(P_{ij}^* - \frac{2}{3} \delta_{ij} P^* \right),$$
$$P_{ij}^* = -\langle u_i u_n \rangle \frac{\partial U_j^*}{\partial x_n} - \langle u_j u_n \rangle \frac{\partial U_i^*}{\partial x_n}, \tag{1.3}$$
$$P^* = -\langle u_m u_n \rangle \frac{\partial U_m^*}{\partial x_n}, \quad \frac{\partial U_m^*}{\partial x_n} = \frac{\partial U_m}{\partial x_n} + \varepsilon_{mpn} \omega_p, \quad E_{ij} = \frac{2}{3} \delta_{ij} \varepsilon,$$

where ε is the rate of dissipation of the total turbulent kinetic energy $k = \langle u_i u_i \rangle / 2$; δ_{ij} is the unit tensor; c_1 and c_2 are empirical constants.

We assume that the velocity of the averaged plane-parallel flow is directed along the x_3 axis, so that $U_1 = U_2 = 0$ and $U_3 = U_3(x_1)$. The flow plane is perpendicular to the axis of rotation and the angular-velocity vector has the components $(0, \omega_2, 0)$. The adopted assumptions entail the discarding of convective-transfer terms in the system (1.1). Neglecting diffusion effects (D_{ij}), we write the algebraic system (1.1) set up, with allowance for (1.2) and (1.3):

$$4\omega_2 \langle u_1 u_3 \rangle + c_1 \frac{\varepsilon}{k} \left(\langle u_1^2 \rangle - \frac{2}{3} k \right) + \frac{2}{3} c_2 \langle u_1 u_3 \rangle \left(\frac{dU_3}{dx_1} - \omega_2 \right) + \frac{2}{3} \varepsilon = 0,$$

$$c_1 \frac{\varepsilon}{k} \left(\langle u_2^2 \rangle - \frac{2}{3} k \right) + \frac{2}{3} c_2 \langle u_1 u_3 \rangle \left(\frac{dU_3}{dx_1} - \omega_2 \right) + \frac{2}{3} \varepsilon = 0,$$

$$2\langle u_1 u_3 \rangle \frac{dU_3}{dx_1} - 4\omega_2 \langle u_1 u_3 \rangle + c_1 \frac{\varepsilon}{k} \left(\langle u_3^2 \rangle - \frac{2}{3} k \right) - \frac{4}{3} c_2 \langle u_1 u_3 \rangle \left(\frac{dU_3}{dx_1} - \omega_2 \right) + \frac{2}{3} \varepsilon = 0, \qquad (1.4)$$

$$\langle u_1^2 \rangle \frac{dU_3}{dx_1} - 2\omega_2 \left(\langle u_1^2 \rangle - \langle u_3^2 \rangle \right) + c_1 \frac{\varepsilon}{k} \langle u_1 u_3 \rangle - c_2 \langle u_1^2 \rangle \left(\frac{dU_3}{dx_1} - \omega_2 \right) = 0,$$

$$k = \left(\langle u_1^2 \rangle + \langle u_2^2 \rangle + \langle u_3^2 \rangle \right) / 2.$$

Introducing the parameter $S = \omega_2 / (dU_3/dx_1)$ and the turbulence scale $l = k^{3/2}/\varepsilon$, from the system (1.4) we obtain

$$k = \alpha l^2 \left(\frac{dU_3}{dx_1} \right)^2 (1 + \beta S + \gamma S^2), \qquad (1.5)$$

$$\langle u_i^2 \rangle = k(a_i + b_i S), \quad -\langle u_1 u_3 \rangle = \alpha^{1/2} k (1 + \beta S + \gamma S^2)^{1/2},$$

$$a_1 = a_2 = \frac{2(c_1 + c_2 - 1)}{3c_1}, \quad a_3 = \frac{2(c_1 - 2c_2 + 2)}{3c_1},$$

$$b_1 = (12 - 2c_2)/3c_1, \quad b_2 = -2c_2/3c_1, \quad b_3 = (4c_2 - 12)/3c_1,$$

$$\alpha = a_1(1 - c_2)/c_1, \quad \beta = [b_1(1 - c_2) + a_1(c_2 - 2) + 2a_3]/[a_1(1 - c_2)],$$

$$\gamma = [b_1(c_2 - 2) + 2b_3]/[a_1(1 - c_2)].$$

We analyze the influence of rotation on the components of the Reynolds stress tensor by taking dU_3/dx_1 and l as constant. The assumption that the turbulence scale is conserved is justified by the fact that the sizes of the energy-bearing vortices are determined mainly by geometrical factors. A similar analysis was made in [8, 9] using different closure models.

We introduce the amount of turbulent energy in the nonrotating stream

$$k_0 = \alpha l^2 (dU_3/dx_1)^2$$

and use it as the scale. In Fig. 1 we present the results of calculations by Eqs. (1.5) in which, as in [7], we took $c_1 = 1.5$ and $c_2 = 0.6$. Curves 1-5 correspond to the dependence on S of the quantities k/k_0, $-\langle u_1 u_3 \rangle / k_0$, $\langle u_1^2 \rangle / k_0$, $\langle u_2^2 \rangle / k_0$, and $\langle u_3^2 \rangle / k_0$.

It is seen that the direct action of rotation on the turbulence is determined primarily by the sign of the parameter S. For $S < 0$ the intensity of the pulsations decreases sharply down to complete disappearance at $S = S^* = -0.069$. It is important to note that for $S < 0$ the relative energy distribution over the components is approximately conserved, while $\langle u_3^2 \rangle \simeq k$. The influence of rotation proves to be more complicated for $S > 0$. At first the intensity of turbulent pulsations increases with an increase in S, with the largest increase being observed for the transverse pulsation $\langle u_1^2 \rangle$. At $S \simeq 0.15$ the quantities k and $-\langle u_1 u_3 \rangle$ reach the maximum values, but the quantity $\langle u_1^2 \rangle$ continues to grow and at $S \simeq 0.2$ it comprises almost half the total energy. With a further increase in S all the components of the pulsation motion decrease, and at $S = S^{**} = 0.373$ they disappear entirely. Thus, the suppression of turbulence is also possible for $S > 0$, although a considerably higher rotation intensity is required in this case than for $S < 0$.
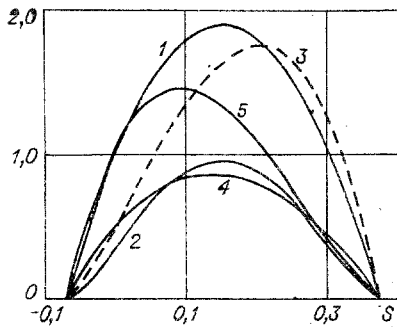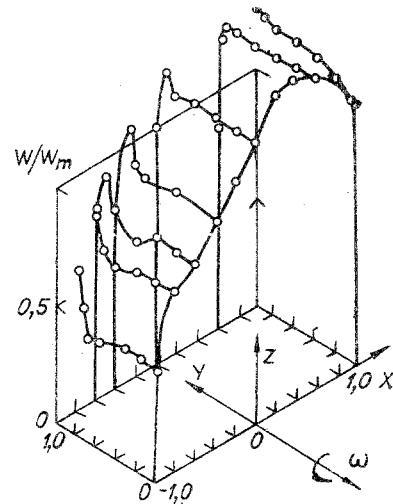
Fig. 1

Fig. 2

2. Experimental Setup

Air flow was investigated in a channel with dimensions of 20 × 20 × 840 mm placed diametrally between two disks. Air entered the channel from a microblower through seals, supply tubes, and a receiver. A honeycomb made of 64 thin-walled tubes 20 mm long and 2.5 mm in diameter was mounted at the entrance to the channel; the ends of the honeycomb were covered with metal grids. Air from the channel was fed to the cavity between the disks, confined on the outside by a continuous rim, and leaked out into the stationary medium through openings near the axis of rotation. A miniature wind tunnel was connected to the suction of the centrifugal blower, serving to calibrate the thermoanemometer sensors and measure the air flow rate while running the tests.

A one-channel, constant-temperature thermoanemometer, placed on the rotating disks, was used to measure the flow characteristics. The output signal of the thermoanemometer, the supply voltages,and the control and monitoring signals were transmitted through a mercury current collector. The thermoanemometer sensor, with a body 1.1 mm in diameter and a holder 6 mm long, had a tungsten filament 5 μm in diameter and 1.0 mm long.

The thermoanemometer signal was recorded and analyzed using a data-measurement complex based on a microcomputer. The experimental installation was built so that none of the electrical connecting lines between the thermoanemometer, the sensor, and the measurement complex were changed in the transition from calibration to running the tests.

The error in maintaining and monitoring the operating parameters is estimated as ±1.3% for the air flow rate through the channel and ±0.5% for the angular velocity of rotation. The total relative error of the measurements (for a confidence coefficient of 0.95) does not exceed 4% for the averaged velocity and 12% for the intensity of pulsations of the longitudinal component. We note that the rms value of the voltage at the thermoanemometer output, connected with the velocity pulsations, exceeded the intrinsic noise of the contacts of the current collector by more than an order of magnitude in the frequency range from 10 to 10,000 Hz.

3. Results of Measurements

As the determining flow criteria we take the Reynolds number $Re = 2W_m h/\nu$ and the complex $K = 2\omega h/W_m$, the reciprocal of the Rossby number. Here h is the channel half-width, W_m is the average flow-rate velocity, and ω is the modulus of the angular velocity vector of rotation. We shall represent the results of the measurements in the coordinate system x, y, z (x_1, x_2, x_3), the z axis of which is directed along the central line of the channel while the y axis is parallel to the axis of rotation. For the dimensionless values of the coordinates, normalized to h, we introduce the designations X, Y, Z (Fig. 2).

The measurements were made for values of Re from 3000 to 9000 and of K from 0 to 0.2. The working cross section was located at a distance Z = 70 from the exist from the honeycomb. It has been established [10] that at this distance from the entrance the stream can be considered as very close to developed, at least with respect to the averaged-velocity fields and the Reynolds stress tensor.
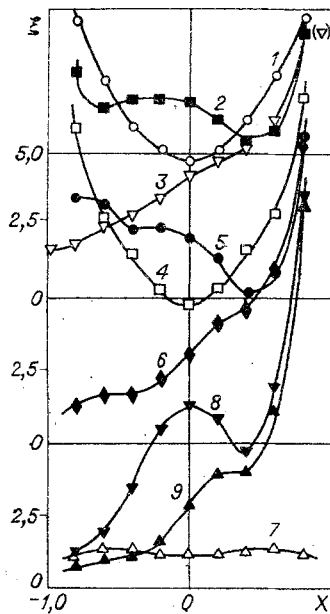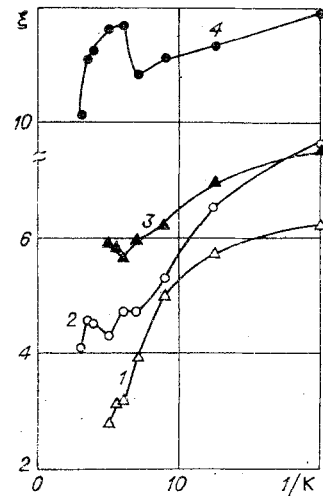
211

Fig. 3

Fig. 4

Special experiments carried out to determine the intensity of secondary flows showed that in all the investigated regimes the angle of deviation of the velocity vector from the channel axis did not exceed several degrees. An exception for $K = O(10^{-1})$ is a thin layer immediately adjacent to the wall on surfaces perpendicular to the axis of rotation. As a consequence of this, the results presented below were obtained with the sensor filament placed transverse to the direction of the main flow.

In Fig. 2 we present the distribution of the averaged longitudinal velocity component in a channel cross section ($\omega_2 = -\omega$) obtained for $Re = 9000$ and $K = 0.2$. The symmetry of the flow relative to the plane $Y = 0$ allows us to confine the measurement to $Y \geq 0$.

It is seen that the velocity maximum is strongly shifted toward the wall running up against the stream (the side with an increased pressure, $X = 1$). A core and thin shear layers on the surfaces perpendicular to the axis of rotation are distinguished in the stream. The layers distinguished are classified as Ekman layers with the determining role of the components of the Coriolis force and the shearing stresses in the balance of forces. At $X \leq 0$ the $W(Y)$ profiles have local maxima, most clearly expressed in the corner regions. A velocity field of this character is also observed in the laminar regime of motion [1].

In Figs. 3-5 we present the results of measuring the quantity $\xi = (\sqrt{<w^2>}/W_m) \cdot 10^2$. The distributions of ξ along the central line $Y = 0$ for nine flow regimes are shown in Fig. 3: 1-3) $K = 0$, 0.025, 0.2, $Re = 9000$; 4-6) $K = 0$, 0.025, 0.2, $Re = 6000$; 7-9) $K = 0$, 0.025, 0.2, $Re = 3000$.

The data obtained at $Re = 3000$, i.e., for the regime with a transitional character of motion in a nonrotating channel, clearly illustrate the destabilizing action of rotation in the region of the stream with $S > 0$. Even a low rotation intensity ($K = 0.025$) causes sharp turbulization of flow in this region.

With an increase in the rotation intensity the effect of suppression of turbulence appears in the region with $S < 0$, and even for $K = 0.2$ the size of the pulsations on the side with the decreased pressure falls to a low level for all values of Re. The character of the variation of ξ as a function of K for several points of the central line $Y = 0$ is shown in Fig. 4 ($Re = 9000$, 1-4: $X = -0.6$, 0, 0.6, 0.8).

In Fig. 5 we present distributions of ξ along several lines parallel to the axis of rotation obtained for $Re = 9000$ (1, 3, 5, 7: $K = 0.08$; 2, 4, 6, 8: $K = 0.2$; dashed lines: $K = 0$; 1, 2; $X = 0$; 3, 4: $X = 0.6$; 5, 6: $X = -0.6$; 7, 8: $X = -0.97$). It is seen that a tendency toward the establishment of a uniform distribution of ξ along lines of $X = $ const with an increase in K is displayed in the core of the stream. This tendency is traced especially clearly in the region adjacent to the side with an increased pressure. The level of pulsations in the Ekman layers near the walls is considerably reduced, on the whole. For example, for $K = $
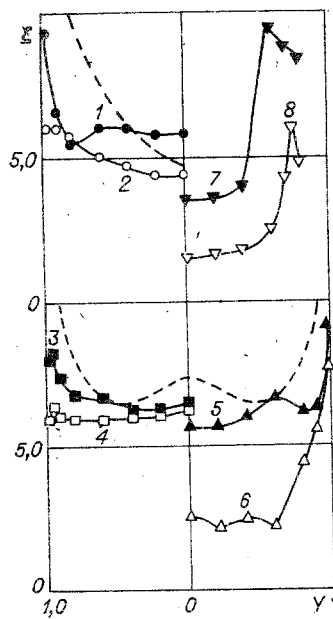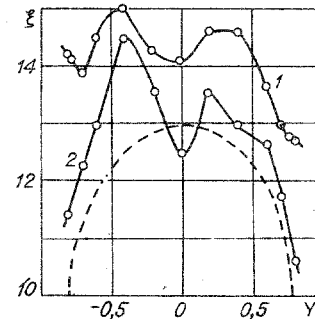
Fig. 5

Fig. 6

0.2 the intensity of pulsations along the line X = 0.6 hardly increases as the wall is approached, which clearly indicates the absence of the generation of turbulence energy in the Ekman shear layer in this regime. A distinctive feature is observed, however, in the distribution of pulsation intensity in the corner regions formed by the side with a decreased pressure (X = —1) and the walls perpendicular to the axis of rotation. The velocity field (see Fig. 2) in this region at a certain distance from the surface has a layer with considerable gradients, in which the intense generation of turbulent energy evidently occurs. As a consequence, local maxima are also formed in the $\xi(Y)$ distribution (see Fig. 5, curves 7 and 8).

The break in curves 2-4 in Fig. 4 at $1/K \simeq 7$ attracts attention. In this connection we note that in an investigation [11] of turbulent flow through a slot channel extending along the axis of rotation the possibility of the formation of large-scale structures with a longitudinal orientation, classified as Taylor—Görtler vortices, against the background of developed turbulent motion at a sufficiently high rotation intensity was established. Similar effects are observed in flows along concave surfaces [12]. In a statistical respect the large-scale structures which form occupy a definite position, adhering to the side with the increased pressure, and their counterinfluence on the main flow is displayed through the action of additional convective transfer with an alternating direction with respect to the wall. Thus, the break in the $\xi(1/K)$ dependences for $X \gtrless 0$ can be interpreted as the onset of the development of Taylor—Görtler vortices. To clarify this question more fully we measured ξ in the transverse direction along the entire wall with an increased pressure in the immediate vicinity of the surface for Re = 9000 and K = 0.2 (Fig. 6, 1: X = 0.97; 2: X = 0.95; dashed line: K = 0, X = 0.97). The thermoanemometer sensor was introduced through the wall X = —1. The two clearly expressed maxima in the $\xi(Y)$ profiles indicate the existence of two pairs of large-scale vortex structures. The maxima in the ξ distribution are smoothed out with greater distance from from the wall. These $\xi(Y)$ profiles are somewhat asymmetrical relative to the point Y = 0. Evidently, this is connected with the high sensitivity of a stream containing Taylor—Görtler vortices to inaccuracies in the construction of the flow channel. We note that when large-scale structures of this type were absent from the stream (for $1/K \gtrless 7$) the degree of symmetry of the velocity fields and the quantity ξ relative to the plane Y = 0 was quite satisfactory.

4. Discussion

The results obtained in the work show that a specific feature of the structure of developed turbulent flow through a rapidly rotating rectangular channel consists primarily in the distinct division of the stream into several regions, characteristic for flows of a rotating fluid. Two of them are identical (by virtue of the flow symmetry) Ekman layers. They are interesting mainly because they make the main contribution to the total surface friction. In fact, the results of measurements of pressure losses in rotating channels and pipes demonstrate

the protraction of the laminar—turbulent transition with an increase in angular velocity [13]. Here the critical values Re_* of the Reynolds number are determined from the start of a sharp change in the character of the dependences of the drag coefficient on the stream criteria. From the results of [14], obtained for a channel with a square cross section, the effect of an increase in Re_* can be determined quantitatively by the empirical formula

$$Re_* = 7 \cdot 10^4 (K + 0.043).$$ (4.1)

Substituting K = 0.2 into (4.1) yields $Re_* = 17,000$, which far exceeds the value of Re = 9000 for which the data in Fig. 5 are given. Consequently, the value of the drag coefficient for Re = 9000 and K = 0.2 indicates motion of a laminar character, whereas in the core of the stream, especially in the region of X > 0, the motion is clearly turbulent. These results can be brought into agreement if the flow in the Ekman layers is considered as laminarized in averaged characteristics and one recognizes their decisive contribution to the hydraulic drag. The absence of a noticeable generation of turbulent energy near the walls (see Fig. 5) supports this conclusion. We note that similar phenomena are displayed in the flow of an electrically conducting fluid through a channel in the presence of a transverse magnetic field [15].

Two other regions make up the core of the stream and differ from each other in the direction of the direct action of the Coriolis force on the turbulence, with the section having a stabilizing action of rotation considerably exceeding in size the section where the opposite effect is displayed. The core as a whole can be characterized as a region in which the main velocity variation occurs in the direction perpendicular to the axis of rotation. Moreover, for $K = O(10^{-1})$ in the range of $-0.7 \leq X \leq 0.2$ both the conditions of plane-parallel flow and of uniformity of shear are approximately satisfied, i.e., the conditions adopted in the semiempirical model of turbulence under consideration. It is interesting that in the dimensionless expression the shear depends weakly on K. On the basis of the experimental data it can be assigned the value

$$\frac{1}{W_m} \frac{dW}{dX} = 0.5 \pm 0.1, \quad -0.7 \leqslant X \leqslant 0.2, \quad K = O(10^{-1}).$$ (4.2)

Comparing (4.2) with the locally determined (S) and the integral (K) parameters of rotation, we write the connection

$$K = -(1.0 \pm 0.2)S.$$ (4.3)

Substituting the value S* = −0.069 into (4.3), we find that in the indicated range of X complete suppression of turbulent pulsations predicted by the model sets in at K* = 0.06-0.08. The data in Fig. 4 (curves 1 and 2) show that the estimate obtained correctly establishes only the order of magnitude of K*; in the tests a sharp decrease in turbulence intensity sets in at values of K exceeding that determined by the model by two to three times.

In a detailed analysis of velocity fields and pulsation characteristics we must not lose sight of convective transfer accomplished by secondary flow, since even at a relatively low level of transverse velocities their transfer action can be appreciable against the background of diffusion processes. In the stream core secondary flow causes a shift of the velocity maximum toward the oncoming wall, while in the Ekman layers it results in dissimilar W(Y) profiles in different cross sections X = const. With respect to the pulsation characteristics, convective transfer by secondary flow inhibits the appearance of effects of the direct action of the Coriolis force on turbulence, on the whole. At a relatively low rotation intensity, when the effect of suppression of turbulence in the region of S < 0 has not yet become decisive, the removal of turbulent energy from the boundary layers to the central part even leads to an increase in the level of ξ relative to the values in a stationary channel (see Fig. 3, curves 2, 5, and 8). It seems that the indicated discrepancy between the theoretical and experimental values of K* for the range of $-0.7 \leq X \leq 0.2$ is due mainly to neglect in the model of the effects of the convective supply of turbulent energy from the region of $-1 \leq X \leq 0.7$, in which the stabilizing action of the Coriolis force is displayed to a lesser degree due to the higher values of dW/dX.

LITERATURE CITED

1. E. M. Smirnov and S. V. Yurkin, "Fluid flow in a rotating channel with a square cross section," Izv. Akad. Nauk SSSR, Mekh. Zhidk. Gaza, No. 6 (1983).
2. J. Moore, "Effects of Coriolis force on the turbulent flow in rotating channels," Report No. 89, Gas Turbine Lab, MIT (1967).

3. A. K. Majumdar, V. S. Pratap, and D. B. Spalding, "Numerical computation of flow in rotating ducts," Trans. ASME, J. Fluids Eng., 99, 148 (1977).
4. R. Simon, R. Schilling, and K. O. Felsch, "Berechnung der ausgebildeten turbulent Strömung in rotierenden Kanälen mit rechteckigem Querschnitt," Stroemungsmech. Stroemungsmasch., No. 28, 33 (1980).
5. J. P. Johnston, "Internal flows," in: Turbulence, P. Bradshaw (ed.), Springer-Verlag, Berlin-New York (1976).
6. J. P. Johnston, R. M. Halleen, and D. K. Lezius, "Effects of spanwise rotation on the structure of two-dimensional fully developed turbulent channel flow," J. Fluid Mech., 56, 533 (1972).
7. B. E. Launder, G. J. Reece, and W. Rodi, "Progress in the development of a Reynolds-stress turbulence closure," J. Fluid Mech., 68, 537 (1975).
8. R. M. C. So, "A turbulence velocity scale for curved shear flows," J. Fluid Mech., 70, 37 (1975).
9. M. M. Gibson, "An algebraic stress and heat-flux model for turbulent shear flow with streamline curvature," Int. J. Heat Mass Transfer, 21, 1609 (1978).
10. V. V. Ris and S. A. Smirnov, "Influence of the entrance conditions on the development of turbulent flow in a rotating channel," in: Structure of Turbulent Flows [in Russian], Minsk (1982).
11. D. K. Lezius and J. P. Johnston, "Roll-cell instabilities in rotating laminar and turbulent channel flows," J. Fluid Mech., 77, 153 (1976).
12. I. A. Hunt and P. N. Joubert, "Effects of small streamline curvature on turbulent duct flow," J. Fluid Mech., 91, 633 (1979).
13. V. K. Shchukin, Heat Exchange and Hydrodynamics of Internal Streams in Mass Force Fields [in Russian], Mashinostroenie, Moscow (1980).
14. E. Döbner, "Über den Strömungswiderstand in einem rotierenden Kanal," Dissertation, Tech. Hochsch. Darmstadt (1959).
15. G. G. Branover and A. B. Tsinober, Magnetohydrodynamics of Incompressible Media [in Russian], Nauka, Moscow (1970).

NUMERICAL STUDY OF LAMINARIZATION EFFECTS IN TURBULENT BOUNDARY
LAYERS OF ACCELERATED FLOWS

V. G. Zubkov

UDC 532.514.4

1. Introduction. In a number of experimental data from studies of turbulent flows with acceleration a substantial variation is noted in the characteritics of heat transfer and friction from the corresponding values, obtained from the relations for turbulent flows [1, 2]. The larger the value of the flow acceleration, the more significant the deviation of the integral characteristics of heat transfer and friction, as well as of the profiles of mean velocities and temperature from the universal relations for the turbulent flow regime toward dependences corresponding to the laminar regime. This effect became called laminarization of turbulent flows.

It is possible to estimate the generation condition of laminarization within the first approximation by means of the acceleration parameter $K = (\nu/U_\infty^2)dU_\infty/dx$, characterizing the extent of flow acceleration. It has been established that lowering of the heat transfer parameters starts being noticed in flows with $K > 2 \cdot 10^{-6}$. This parameter, however, does not allow quantitative estimation of effects generated by laminarization.

Account of the variation in the structure of turbulent flows under the action of accelerated flow makes it possible to approach more correctly the projection of various constructions. For example, for an external flow, when the gas flow between turbine blades and in supersonic nozzles an inverse flow transition can cause lowering of heat transfer between the heating gas flow and the construction surface. In heat transfer instruments, when the heat transfer intensity must be largest, a similar effect leads to undesirable results. This gen-